Geriatric Orthopaedic Surgery
& Rehabilitation
Volume 11: 1-9

DOI: 10.1177/2151459320956958
journals.sagepub.com/home/gos
SAGE

Role of Additional Inferomedial Supporting Screws in Osteoporotic 3-Part Proximal Humerus Fracture: Finite Element Analysis

Hyojune Kim, MD[1,*], Wonhee Lee, MS[2,*], SeungHyun Choi, MS[2], Erica Kholinne, MD, PhD[1,3], Euisop Lee, MD[1], Wael Mohammed Alzahrani, MD[1,4], Kyoung Hwan Koh, MD, PhD[1], In-Ho Jeon, MD, PhD[1], and Shinseok Kim[1]

Abstract

Introduction: Importance of inferomedial supporting screws in preventing varus collapse has been investigated for the proximal humerus fracture. However, few studies reported the results of osteoporotic complex fracture. This study aimed to demonstrate the stress distribution pattern, particularly in osteoporotic 3-part proximal humerus fractures involving greater tuberosity (GT) with different screw configurations. **Materials and methods:** Using the computed tomography (CT) images of 2 patients, who had osteoporosis and the other had normal bone density, 3-part fractures involving the GT, without medial support were reconstructed. To reflect the osteoporosis or real bone density, Hounsfield unit of CT scans were utilized. A force of 200 N was applied in 30° varus direction. The proximal screws were set in 2 ways: 6 screws without inferomedial supporting screws and 9 screws with inferomedial supporting screws. Qualitative and quantitative analysis of internal stress distribution were performed. **Results:** The most proximal part area near humeral head vertex and near the 1st screw's passage and tip had more stress concentrated in osteoporotic 3-part fractures. The stress distribution around the proximal screws was found near the GT fracture line and its lateral side, where the local max values located. Inferomedial supporting screws decreased these effects by changing the points to medial side from the GT. The ratio in osteoporotic bone model decreased to that in normal bone model when inferomedial supporting screws were applied (normal bone, 2.97%–1.30%; osteoporosis bone, 4.76%–1.71%). **Conclusions:** In osteoporotic 3-part proximal humerus fracture, the stress distribution was concentrated on the area near the humeral vertex, 1st row screw tips, and lateral side region from the GT fracture line. Moreover, inferomedial supporting screws ensured that the stress distribution is similar to that in normal bone setting, particularly in osteoporotic condition.

Keywords

proximal humerus fracture, 3-part fractures, osteoporosis, finite element analysis, the most proximal screw, inferomedial supporting screw

Submitted July 7, 2020. Revised August 8, 2020. Accepted August 18, 2020.

Introduction

Proximal humerus fractures (PHF) occur frequently and the incidence is increasing owing to the rising rates of osteoporosis and increasing life expectancy.[1] Fractures of the proximal humerus account for 5% of all fractures, with a high prevalence in elderly patients.[2,3] For displaced PHF, open reduction-internal fixation is performed most often by use of locking plates to restore shoulder function.[4] These locking plate systems have transformed the treatment of PHF dramatically by reducing mechanical failures. However, despite their use, failure rates still remain as high as 35%. This is due to

[1] Department of Orthopaedic Surgery, Asan Medical Center, University of Ulsan College of Medicine, Seoul, Korea
[2] Anymedi Inc, Seoul, Korea
[3] Department of Orthopedic Surgery, St. Carolus Hospital, Jakarta, Indonesia
[4] Department of Orthopaedic Surgery, Najran University Hospital, Najran, Saudi Arabia
* Co-first author

Corresponding Author:
In-Ho Jeon, MD, PhD, Department of Orthopaedic Surgery, Asan Medical Center, University of Ulsan, 88, Olympic-ro 43-gil, Songpa-gu, Seoul 05505, Korea.
Email: jeonchoi@gmail.com

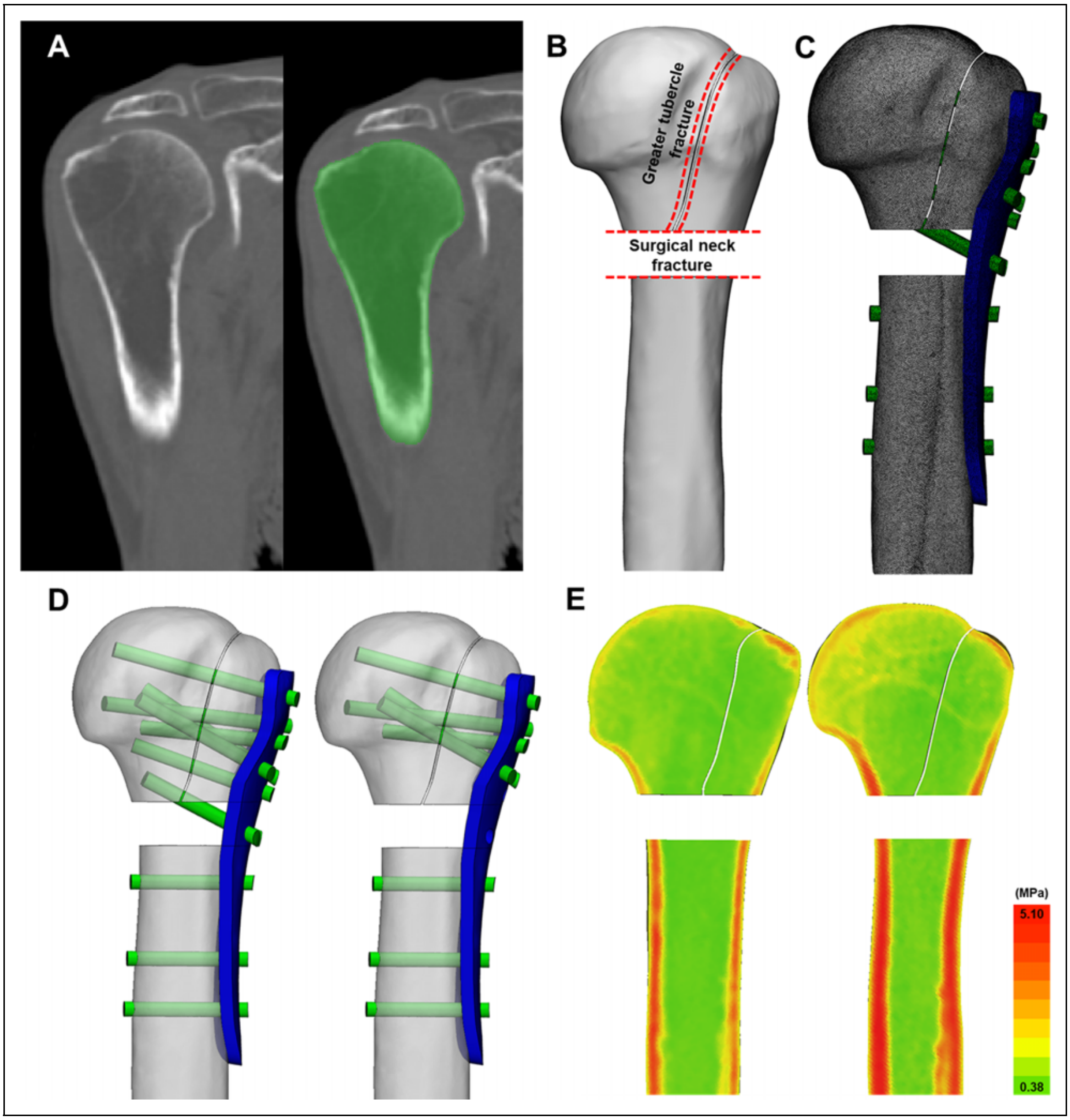

Figure 1. (A): Humerus bone segmentation based on CT DICOM files. 3D modeling is performed by first masking the area. (B): Humeral fracture design based on the 3D model. Surgical neck fracture and anatomical neck fracture were formed to create a 2-part fracture and 3-part fracture model, respectively. (C): Mesh structure for finite element analysis. The surface is a triangular mesh type and the volume mesh is conducted with the tetrahedral structure. (D): A screw and plate design according to the 3-part fracture was designed to fit perfectly with the bone; 9- and 6-screw models were applied above the surgical neck. (E): Elastic modulus distribution of osteoporotic and normal bone. Each elastic modulus was entered for each element according to the CT DICOM HU value.

complications such as secondary varus collapse, reduction loss, screw penetration or perforation, and osteonecrosis.[5-8] To reduce mechanical failure rates, some studies found that medial region mechanical support is important for preventing secondary reduction loss when PHFs are treated with locking plates.[9] Studies have shown that placing inferomedial support locking screws is an important technique, particularly in patients with medial comminution, which was common in osteoporotic fracture.[10-12]

Furthermore, complex fractures combined with osteoporosis were indicated as poor prognostic factors that could easily lead to loss of reduction and subsequently result in mechanical failure after internal fixation.[13,14] The mechanical complications were shown to increase, especially in patients with osteoporosis and complex fractures, such as Neer 3- and 4-part fractures.[13] However, complications associated with the complex fractures were not completely evaluated, considering the stress distribution around the proximal screws applied with the locking plate.

Locking plates have 7 to 9 screw holes for proximal fragments. Recently, studies have sought to identify the most appropriate screw configuration and plate position in proximal humerus fracture.[5,15,16] However, there is no consensus on the optimal number and location of screws specifically for patients with osteoporosis and complex PHF.

Therefore, the aim of the current study was to investigate the stress distribution in osteoporotic complex fractures and

Table 1. Bone, Metal Plate, and Screw Property Equations.

	Bone densityDensity: ρ (kg/m^2)	Elastic modulus: *E* (*MPn*)	Poisson's ratio: *v*
Bone	$\rho = 527 + 0.44$ HU	$E = 1049.25 \times 10^{-6} \times \rho^2$ ($\rho \leq 350$ kg/m^3)	0.3
Plate		E = 110.000	0.35
Screw			

compare them with normal bone density according to screw configurations. Our prime focus was the effect of osteoporosis and complex fracture. We hypothesized that (1) stress concentration in area near the 1st row screw tips could be aggravated in osteoporotic 3-part fracture and (2) applying additional inferomedial supporting screw at osteoporotic 3-part fracture would make the stress distribution of proximal humerus be similar to that in normal bone.

Methods

The Institutional Review Board approved this study (AMC IRB N 2019-0015). We conducted the current study in compliance to the 1964 Helsinki declaration and its later amendments or comparable ethical standards. We chose 2 patients, one with normal bone density who was a 38-year-old female without comorbidities and the other was an 81-year-old female with osteoporosis (BMD -4). Both patients were examined by computed tomography (CT). Neither of the patients had humeral deformities, arthritic changes, or fractures.

Image Segmentation

Image segmentation of the proximal humerus bones were built based on the CT scans as DICOM files, using slices less than 1 mm in thickness and a high resolution of 512 × 512 pixels using Materialise Mimics 22.0 software (Materialise, Leuven, Belgium) (Figure 1A). 3D reconstructed images containing both cortical and trabecular bone were formed from extracted the images, which were subsequently transformed into STL files.

Bone, Plate, and Screw Model Reconstruction

Using the 3-Matic 14.0 software (Materialise, Leuven, Belgium), 3D reconstructed images were re-set according to fracture patterns (Figure 1B). We represented the fractures in the models through virtual osteotomies. We created a 3-part proximal humerus fracture model in 2 steps. Firstly, we modeled a surgical neck fracture by forming a 10 mm gap in the intact model. Finally, we created a greater tuberosity (GT) fracture separated by a 0.5-mm gap (11-B3.2 or 11-B2.3 fractures, Figure 1B).

A PHILOS plate (Depuy Synthes, Zuchwil, Switzerland) and screws were scanned using a 3D scanner C-500 (Medit, South Korea) and transformed into STL files to create a 3D reconstructed bone model. The surface between the plate and bone was assumed to be completely in contact, but not in inference of each other. Following surgical techniques implemented for AO, the plate was aligned with the bone's long axis, positioned 4 mm distal to the superior aspect of the greater tubercle, which was the most stable and fixable orientation based on previous study.[16] We modeled the distance from the surface of the subchondral bone to the screw tip at 4 mm to reduce the risk of mechanical cut-out failure.[15] The distal screw, which was applied to the bone near the neck cutting area, was set in a vertical position to the mechanical axis of the humeral shaft. We modeled distal screws with a screw length of 2 mm longer from the distal cortical bone surface (Figure 1C).[15]

Mesh Operation and Material Properties

The FE models of bone, plate and screws were meshed with trihedral elements of surface mesh with a side length 0.5 mm. Volumetric meshes were generated as tetrahedral elements. The completed bone mesh model was extracted with Materialize Mimics 22.0 software to calculate the material property values before applying them to the fine element analysis (FEA) solver. The plate and screw models were then extracted to fit into the FEA solver (Figure 1D and E).

Material properties were assumed to be linear elastic and simulated titanium alloy for the implant components of plate and screws, with Young's modulus of 110 GPa and a Poison's ratio of 0.35 (Table 1).[17] The extracted bone models were linear elastic, with bone element stiffness based on BMD values sourced from the CT scans using Hounsfield units (HU) of previous studies (Table 1).[18-21]

Each participant's bone mineral density was calculated using the formula for calculating bone density based on CT Hounsfield unit (HU) values from the existing studies.[22] The equation for calculating the elastic modulus from bone density was also used based on previous study. The Poisson ratio of bone was used based on existing values. Since the metal plate and screws were made of titanium, the elastic modulus and Poisson ratio were used with reference to the intrinsic properties of titanium materials.[17]

Implementing Basic Principles of the Finite Elements Model

A loading test was performed using the Hyperworks Hypermesh 12.0 (Altair Engineering Inc, USA) FEA solver. A varus force was also applied with the humerus abducted in a 30-degree neutral position, which was considered the physiologic loading mode's position (Figure 2A).[15,23] The 200 N of force was loaded based on a previous study that showed material properties are maintained in a linear relation to loading until 200 N. All mesh used demonstrated isotropic, linearly elastic behavior.[24]

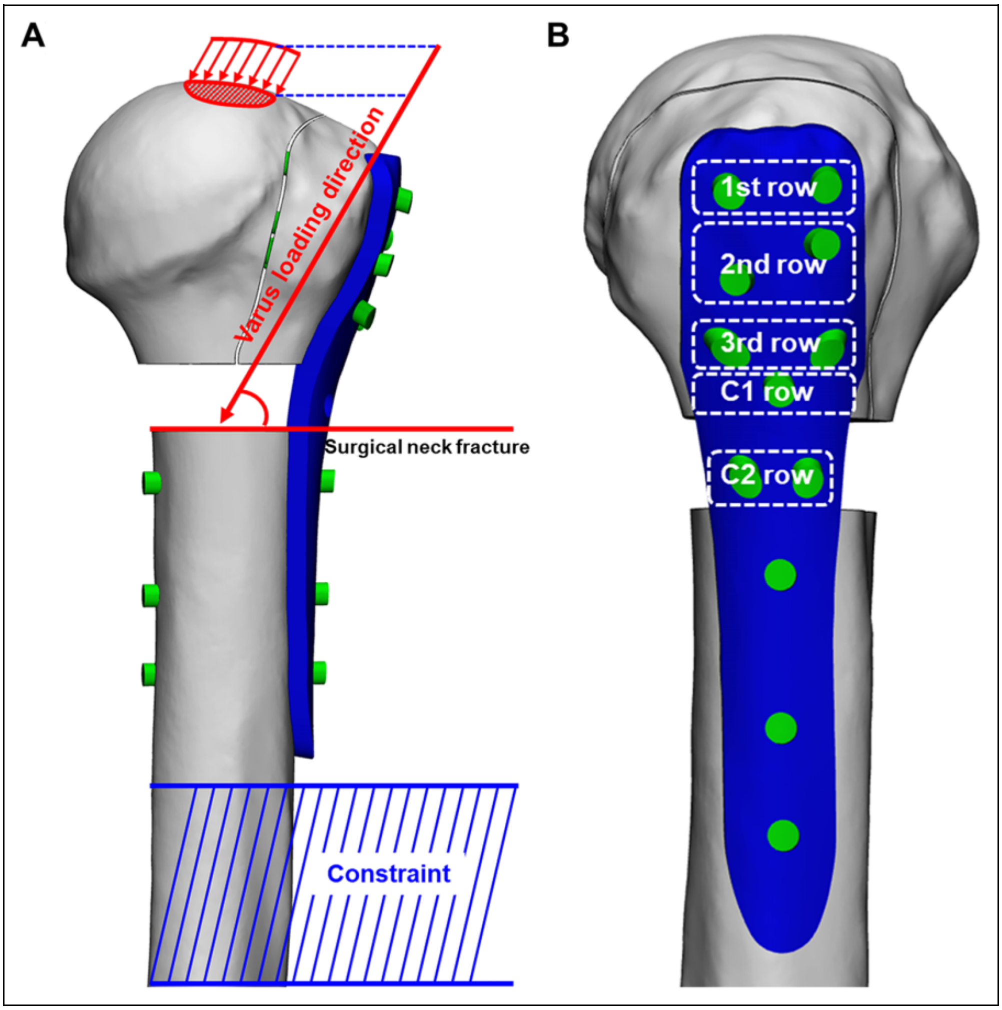

Figure 2. Varus loading setting for the finite elements model (A) Finite elements model for varus loading. Varus loading was applied to the top of the humerus cartilage region in a direction 30 degrees to the surgical neck fracture line. Both axial and varus loading were applied to the same area. (B): Screw column separation for analysis.

Analysis

Based on the biomechanical analysis, cartilage was damaged by octahedral shear stress which is related to osteoarthritis progression as revealed in previous studies.[25] We analyzed the stress distribution using von Mises stress parameters, since this stress is similar to that seen with cartilage damage, except for the octahedral shear stress and modulus. For detailed analysis, each proximal screw row was divided into 5 rows, and each stress distribution was shown by measuring contour map and local max stress values (Figure 2B). We used the 2 different variables to evaluate the stress distribution according to the following points. Firstly, we compared a 6-screw model (without inferomedial supporting screws group) with a 9-screw model (with inferomedial supporting screws group). Secondly, we compared the osteoporosis group with the normal bone group.

In our context, we performed analyses in the following steps. Firstly, we performed qualitative analyses of the proximal humerus segment. Secondly, we analyzed local maximum values around the proximal screws. Finally, we performed semiquantitative analysis to evaluate the stress element ratios in the proximal humerus segment. Before analyzing using the semiquantitative method, we calculated the local maximum stress values. Overall, 0.865 MPa was found to be the lowest value of the local maximum screw stress. Thus, we set this value as reference to investigate the relative stress element ratios.

Results

Qualitative Analysis of Proximal Humerus: Most Proximal Part and GT Line

Compared with normal bone, the stress distribution in osteoporotic bone model was more concentrated near the humeral vertex and 1st row screws' passage and tip. The stress distribution decreased when inferomedial supporting screws were

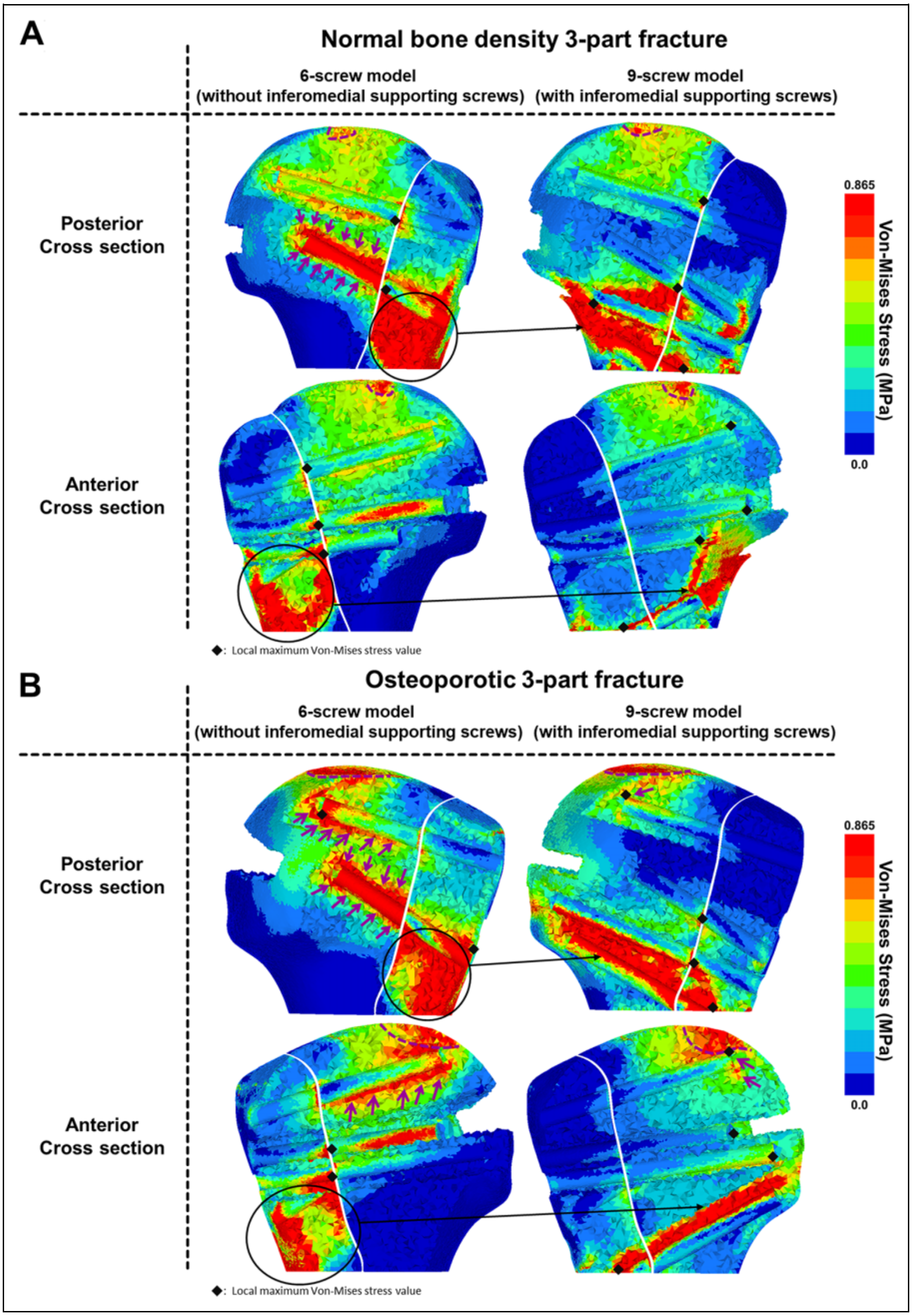

Figure 3. Von Mises stress distribution of (A) normal bone and (B) osteoporosis during varus loading. The most proximal screws of the osteoporotic bone had a greater stress distribution in the screw passages and tips compared to normal bone (purple arrow). The differences were more pronounced, especially in the humeral cartilage region (purple dotted line, - - -). When we applied the calcar screws, the stress distribution located in lateral position moved to the medial position (black circle with black arrow, O). The local maximum screw value in the osteoporotic bone occurred mostly at the screw tip. Meanwhile in normal bone, it occurred mostly at the intersection point of the GT fracture line and the screws (diamond dotted, ♦).

applied. However, in the osteoporotic bone setting, the stress concentrated near the humeral vertex was found to be still higher than 0.865 MPa.

Stress concentration where the screws crossed the GT fracture line was prominent in both normal and osteoporotic bone models. In the area caudal to the most distal part of the

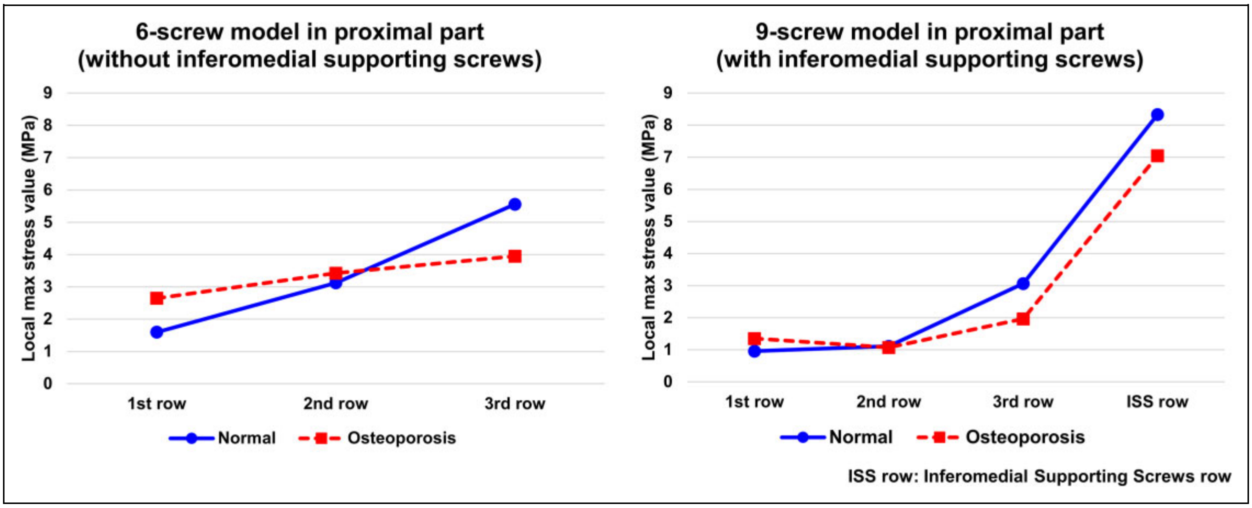

Figure 4. The graph of local max value acting on the screw passage for each number of screws. The local max value of first row screws was higher in osteoporotic fracture than in normal bone density fracture. However, adding inferomedial supporting screws lowered the overall stress concentration of first, second, and third row screws with a pattern similar to that of normal bone.

Table 2. Stress Elements Ratio More Than 0.865 MPa in the Proximal Head Region.

Percentage	Loading	Normal	Osteoporosis
6-screws	Varus	2.97	4.76
9-screws	Varus	1.30	1.71

proximal screws, the stress was distributed from the GT line toward the lateral aspect of the bone (6-screw model, without inferomedial supporting screw groups). We noted this distribution pattern in normal and osteoporotic bone models. In the 9-inferomedial supporting screw model, the stress distribution pattern was different. Here, the stress concentration moved medially from the GT line (9-screw model, with inferomedial supporting screw groups).

Local Maximum Values Around Proximal Screws

In the 6-screw model, the stress was concentrated in the third row, and the local maximum stress value appeared along the GT line. In the case of osteoporosis, the stress was concentrated not only in the third row but also on the vertex cartilage side and first screw's tip side. Conversely, on using the inferomedial supporting screw, the stress concentrated on the lateral distal aspect of the GT line shifted to the medial side. Then, the stress is distributed between the inferomedial supporting screws and the periphery. Accordingly, we found the location of local maximum stress value on the medial side of the GT line, where the screw tips were located.

In both the bone models, on application of inferomedial supporting screws, the local maximum stress values near the GT line declined for every row's screw. The local maximum stress values near the inferomedial supporting screws peaked at all proximal screws (osteoporosis: 7.05 MPa and normal: 8.33 MPa) (Figure 4). Using the 6 screws (without inferomedial supporting screw), we observed that the stress was relatively higher at the first screw in osteoporosis (osteoporosis: 2.65 MPa and normal: 1.60 MPa). Conversely, the local maximum stress value was similar between normal and osteoporosis bones on using the 9-screw model (including inferomedial supporting screws: osteoporosis: 1.35 MPa and normal: 0.96 MPa). On application of the inferomedial supporting screw, the local max value in the first screw row dropped to a relatively similar level for normal bone.

Semiquantitative Analysis of Stress Elements Ratio

Considering the ratios based on >0.865 MPa, inferomedial supporting screw insertion led to a decrease in the ratio (normal bone, 2.97%–1.30%; osteoporosis bone, 4.76%–1.71%) (Table 2). Especially in osteoporosis, the stress distribution changes evenly.

Discussion

We evaluated the internal stress distribution in plating on the 3-part proximal humerus fracture model by comparing normal bones with osteoporosis according to existence of inferomedial supporting screws. We hypothesized that stress concentration on area near the first row screw tips could be aggravated in osteoporotic 3-part fracture. In addition, applying additional inferomedial supporting screw at osteoporotic 3-part fracture would make the stress distribution of proximal humerus similar to that of normal bone

We found that the stress was relatively concentrated near the most proximal humerus region (vertex and 1st screw row's passage and tip) in osteoporosis model compared with normal bone. This concentration declined when inserting the inferomedial supporting screws, which was more prominent in the osteoporotic model. In addition, the medial part of inferomedial supporting screws showed the most concentrated region.

Furthermore, inferomedial supporting screws reduced the stress distribution in proximal humerus part, almost similar to normal bone setting. Therefore, our hypotheses were validated.

One of our hypotheses was proven by our descriptive results of internal stress and relatively more proportion on the proximal humerus region: humeral vertex and first row screws' passage and tips. In the osteoporosis compared with normal model, stress concentration near the most proximal screw was dominantly distributed at the screw's tip and screw's undersurface. Although these regions decreased on application of inferomedial supporting screws, humeral head vertex region remained as high stress concentrated region. When using internal fixation with a plate in the proximal humerus fracture, there have been reports of clinically poor outcomes with functional loss due to cut-through or cut-out of screws in the proximal head articular side.[12] In particular, when mechanical complications such as cut-out of screws occurred in the humeral head articular cartilage area, poor prognosis could be expected. In the absence of medial support, it was assumed to be vulnerable to varus deformity owing to a lack of inner support. However, no objective basic study has been conducted on this phenomenon. In this study, when a varus force was applied to a fracture without medial support, a significant stress concentration was observed at the vertex area of the humeral head and 1st screw's region in the osteoporosis versus the normal model. Based on these results, the osteoporotic 3-part fracture including the GT site is vulnerable to varus deformity force and more susceptible to screw cut-out. Therefore, it is more important to prevent screw cut-out complications by inferomedial supporting screw fixation if a patient with osteoporosis has a 3-part fracture.

On comparing the proximal 6-screw and 9-screw model, it was clear that the inferomedial supporting screw's role was to decrease the proximal humeral head stress by lengthening the working length of the proximal screws. The working length of a constructed plate is defined as the distance between the first screws on either side of the fracture.[26] We noticed that the distance between the most proximal and distal screws (working length) was longer in the 9-screw model. To the best of our knowledge, no previous reports showed the most optimal working length for PHF. Nevertheless, Fletcher et al showed that stable fixation for a proximal humerus fracture is based on the screw's configuration and a longer distance between screws in the proximal part was important for rigid fixation.[5]

In addition, we found that inferomedial supporting screws in 3-part (involving GT) PHF could reduce stress on fracture sites near the GT and had supporting roles. This was gleaned from our descriptive finding of internal stress distribution patterns and localized max value location. The stress distribution near the fracture site of GT was transferred to the medial bone area on application of inferomedial supporting screws. The inferomedial supporting screw is known to strengthen the medial cortex support, and it may play an important role in osteoporotic fractures with comminution.[12] However, no reports exist on how inferomedial supporting screws reduce stress in the GT area. Although the role of inferomedial supporting screws can be inferred from previous studies, our reports suggest that it is necessary to apply inferomedial supporting screws for 3-part fractures to reduce the stress on the GT fracture sites and increase the bone union of GT.

Similarly, the stress element ratio of the proximal head region in osteoporosis, based on the elements of >0.865 MPa, declined in the normal bone on application of inferomedial supporting screws compared with that in the other regions of the proximal humerus. Previous reports show that internal fixation of the proximal humerus significantly reduces mechanical complications on application of inferomedial supporting screws.[27] Moreover, our study showed that the inferomedial supporting screws played a role in the 3-part proximal humerus fracture by reducing the stress near the proximal humerus. Furthermore, the effect was more prominent in the osteoporosis group. Therefore, it is important to achieve stress distribution conditions similar to that of normal bone in patients with osteoporosis by ensuring a strong fixation force in the inferomedial region, positioned by inferomedial supporting screws.

The strength of our study is that we made the finite elements models using real patients' CT data, including information of bone density. We also used calculation methods that could reflect the osteoporotic bone mechanical properties indirectly by obtaining HU from the CT images. Therefore, it was possible to evaluate the stress distribution in the setting of fractures among patients with osteoporosis.

However, this research has some limitations. First, our findings could not be applied to the general population because of the small number of cases. However, we used the real patient data, through finite element analysis, and the setting was controlled to prove the specific effects that may be applied in a clinical setting. Secondly, we did not consider the musculotendinous force effect around the glenohumeral joint, which is a limitation of FEM studies. This means the results do not reflect the non-linear properties of soft tissue.

Conclusion

In osteoporotic 3-part proximal humerus fracture, the stress distribution was concentrated on the area near the humeral vertex, 1st row screw tips, and lateral side region from the GT fracture line. Moreover, inferomedial supporting screws should be applied in osteoporotic condition to ensure that the stress distribution is similar to that in a normal bone setting.

Authors' Note

Co-first author: Hyojune Kim, MD, Wonhee Lee, MS. All data included in this study could be accessible.

Acknowledgments

The authors would like to thank Enago for the English language review.

Declaration of Conflicting Interests

The author(s) declared no potential conflicts of interest with respect to the research, authorship, and/or publication of this article.

Funding

The author(s) disclosed receipt of the following financial support for the research, authorship, and/or publication of this article: This study was supported by a grant (2020IE0014) from the Asan Institute for Life Sciences, Asan Medical Center, Seoul, Korea. IRB number: AMC N 2019-0015. Research was supported from Asan Medical Center, as selected (2020IE0014-1).

ORCID iD

Kyoung-Hwan Koh, MD, PhD https://orcid.org/0000-0002-6181-9621

References

1. Bahrs C, Tanja S, Gunnar B, et al. Trends in epidemiology and patho-anatomical pattern of proximal humeral fractures. *Int Orthop*. 2014;38(8):1697-1704.
2. Bell JE, Leung BC, Spratt KF, et al. Trends and variation in incidence, surgical treatment, and repeat surgery of proximal humeral fractures in the elderly. *J Bone Joint Surg Am*. 2011; 93(2):121-131.
3. Launonen AP, Lepola V, Saranko A, Flinkkilä T, Laitinen M, Mattila VM. Epidemiology of proximal humerus fractures. *Arch Osteoporos*. 2015;10(1):209.
4. Tepass A, Blumenstock G, Weise K, Rolauffs B, Bahrs C. Current strategies for the treatment of proximal humeral fractures: an analysis of a survey carried out at 348 hospitals in Germany, Austria, and Switzerland. *J Shoulder Elbow Surg*. 2013;22(1): e8-14.
5. Fletcher JW, Windolf M, Richards RG, Gueorguiev B, Varga P. Screw configuration in proximal humerus plating has a significant impact on fixation failure risk predicted by finite element models. *J Shoulder Elbow Surg*. 2019;28(9):1816-1823.
6. Seide K, Triebe J, Faschingbauer M, et al. Locked vs. unlocked plate osteosynthesis of the proximal humerus—a biomechanical study. *Clin Biomech (Bristol, Avon)*. 2007;22(2):176-182.
7. Hardeman F, Bollars P, Donnelly M, Bellemans J, Nijs S. Predictive factors for functional outcome and failure in angular stable osteosynthesis of the proximal humerus. *Injury*. 2012;43(2): 153-158.
8. Kralinger F, Blauth M, Goldhahn J, et al. The Influence of local bone density on the outcome of one hundred and fifty proximal humeral fractures treated with a locking plate. *J Bone Joint Surg Am*. 2014;96(12):1026-1032.
9. Sproul RC, Iyengar JJ, Devcic Z, Feeley BT. A systematic review of locking plate fixation of proximal humerus fractures. *Injury*. 2011;42(4):408-413.
10. Gardner MJ, Weil Y, Barker JU, Kelly BT, Helfet DL, Lorich DG. The importance of medial support in locked plating of proximal humerus fractures. *J Orthop Trauma*. 2007;21(3): 185-191.
11. Oppebøen S, Wikerøy AK, Fuglesang HF, Dolatowski FC, Randsborg PH. Calcar screws and adequate reduction reduced the risk of fixation failure in proximal humeral fractures treated with a locking plate: 190 patients followed for a mean of 3 years. *J Orthop Surg Res*. 2018;13(1):197.
12. Padegimas EM, Chang G, Namjouyan K, Namdari S. Failure to restore the calcar and locking screw cross-threading predicts varus collapse in proximal humerus fracture fixation. *J Shoulder Elbow Surg*. 2020;29(2):291-295.
13. Gerber C, Werner CM, Vienne P. Internal fixation of complex fractures of the proximal humerus. *J Bone Joint Surg Br*. 2004; 86(6):848-855.
14. Cho CH. Is Minimal invasive plate osteosynthesis a viable treatment option for 4-part proximal humerus fractures? *Clin Shoulder Elbow*. 2018;21(4):177-178.
15. Fletcher JW, Windolf M, Grünwald L, Richards RG, Gueorguiev B, Varga P. The influence of screw length on predicted cut-out failures for proximal humeral fracture fixations predicted by finite element simulations. *Arch Orthop Trauma Surg*. 2019;139(8): 1069-1074.
16. Fletcher JW, Windolf M, Richards RG, Gueorguiev B, Buschbaum J, Varga P. Importance of locking plate positioning in proximal humeral fractures as predicted by computer simulations. *J Orthop Res*. 2019;37(4):957-964.
17. Feerick EM, Kennedy J, Mullett H, FitzPatrick D, McGarry P. Investigation of metallic and carbon fibre PEEK fracture fixation devices for three-part proximal humeral fractures. *Med Eng Phys*. 2013;35(6):712-722.
18. Nam KH, Seo I, Kim DH, Lee JI, Choi BK, Han IH. Machine learning model to predict osteoporotic spine with hounsfield units on lumbar computed tomography. *J Korean Neurosurg Soc*. 2019; 62(4):442-449.
19. Nappo KE, Christensen DL, Wolfe JA, Tintle SM. Glenoid neck Hounsfield units on computed tomography can accurately identify patients with low bone mineral density. *J Shoulder Elbow Surg*. 2018;27(7):1268-1274.
20. Gausden EB, Nwachukwu BU, Schreiber JJ, Lorich DG, Lane JM. Opportunistic use of CT imaging for osteoporosis screening and bone density assessment: a qualitative systematic review. *J Bone Joint Surg Am*. 2017;99(18):1580-1590.
21. Choi MK, Kim SM, Lim JK. Diagnostic efficacy of Hounsfield units in spine CT for the assessment of real bone mineral density of degenerative spine: correlation study between T-scores determined by DEXA scan and Hounsfield units from CT. *Acta Neurochir (Wien)*. 2016;158(7):1421-1427.
22. Gupta S, Van Der Helm FC, Sterk JC, Van Keulen F, Kaptein BL. Development and experimental validation of a three-dimensional finite element model of the human scapula. *Proc Inst Mech Eng H*. 2004;218(2):127-142.
23. Čukelj F, Knezević J, Kodvanj J, et al. Computer representation of osteosynthesis stability in locking plates used for the treatment of osteoporotic proximal humerus fractures. *Psychiatr Danub*. 2014; 26(suppl 2):370-375.
24. Zhang YK, Wei HW, Lin KP, Chen WC, Tsai CL, Lin KJ. Biomechanical effect of the configuration of screw hole style on locking plate fixation in proximal humerus fracture with a simulated gap: a finite element analysis. *Injury*. 2016;47(6):1191-1195.
25. Carter DR, Beaupré GS. *Skeletal Function and Form: Mechanobiology of Skeletal Development, Aging, and Regeneration*. Cambridge University Press; 2007.

26. Hoffmeier KL, Hofmann GO, Mückley T. Choosing a proper working length can improve the lifespan of locked plates. a biomechanical study. *Clin Biomech (Bristol, Avon)*. 2011;26(4): 405-409.

27. Padegimas EM, Zmistowski B, Lawrence C, Palmquist A, Nicholson TA, Namdari S. Defining optimal calcar screw positioning in proximal humerus fracture fixation. *J Shoulder Elbow Surg*. 2017;26(11):1931-1937.